

AN ULTRAFAST THERMAL EMISSION SPECTROMETER
FOR INVESTIGATING TEMPORAL THERMAL EMISSION OF METAL THIN-FILMS
AND THEIR REACTIVE DERIVATIVES

BY

ALEXANDER KNIGHT MOORE

THESIS

Submitted in partial fulfillment of the requirements
for the degree of Master of Science in Chemistry
in the Graduate College of the
University of Illinois at Urbana-Champaign, 2018

Urbana, Illinois

Adviser:

Professor Dana Dlott

ABSTRACT

An experimental system was constructed for studying the reaction of nanolaminate thermites in both the temporal and spectral domains. 1mJ pulses from a Ti:Sapphire laser, stretched to 10ps, were focused onto sample films affixed to glass slides. The emission generated by the ablation of the films was collected and focused into a spectrograph and subsequently directed into a Hamamatsu C4334 streak device. It was found that this system was capable of providing spectral and temporal information from the emission of ablated metal and thermite nanolaminate films over a timescales ranging from tens of nanoseconds to milliseconds.

*There once was a man, and he's me
Who wished much to complete his degree
So he wrote all this stuff
And he hopes it's enough
To convince you to let him go free!*

Acknowledgements

I'm tremendously grateful to my Advisor Dana Dlott, as well as Sergey Matveev for their guidance and support.

Table of Contents

List of Figures	-----	vi
Chapter 1	Introduction	1
Chapter 2	Materials and Methods	2
2.1	Laser System	2
2.2	Ti:Sapphire Oscillator	2
2.3	Chirped Pulse Amplification (CPA) System	2
2.4	Stretcher	3
2.5	Regenerative Amplifier (RGA)	3
2.6	Multipass Amplifier (MPA)	4
2.7	Experimental Design	5
2.8	Timing Schemes	6
2.9	Time Profiling	9
2.10	Sample Preparation	11
Chapter 3	Results and Discussion	13
References	-----	15

List of Figures

1	Laser Layout -----	5
2	Experimental Layout -----	6
3	Trigger Scheme A -----	7
4	Trigger Scheme B -----	8
5	Trigger Scheme C -----	9
6	Autocorrelator Layout -----	10
7	Autocorrelation of Partially Compressed Beam -----	11
8	Profile of Thick Zr Film -----	12
9	Profile of Thin Zr Film -----	12
10	Typical Streak Image -----	14
11	Comparison of Emission Time Profiles -----	14

Chapter 1

Introduction

Thermite reactions, which consist of an early transition metal fuel and a late transition metal oxide oxidizer, are of interest within the energetic materials community, as they can release more energy than can conventional molecular explosives. Of particular interest is the process by which thermite reactions are initiated at the interfaces between the fuel and oxidizer. Several studies have investigated the role of the interfacial region between metal fuel and oxidizer in the thermite reaction by using systems consisting of alternating nm-scale layers of metal and metal oxide deposited by sputtering.^{1,2} Such systems are known as nanolaminate thermite. The initiation of thermite has been studied in several different ways. Thermite systems have been heated in stages with gravimetric analysis, heated rapidly using a filament, and initiated mechanically by using the laser driven flyer plate system developed by the Dlott group.^{1,2,3} Another interesting means of initiating thermite would be to heat them rapidly using a ps laser pulse. Here, a system is described capable of initiating nanolaminate thermite in this way, and collecting time-resolved spectral information from the thermal emission of the resulting reaction. A Zr:CuO system was selected as a model system because Zr possesses an exceptionally high oxygen diffusion rate which increases the ease of initiating the reaction in our system.

Chapter 2

Materials and Methods

2.1 Laser System

A Ti:Sapphire laser system was used to generate pulses for ablating metal films and initiating thermite samples. The system consisted of a passively mode-locked laser oscillator, which was the source of the ultrashort pulses. Following the oscillator, the laser pulses were amplified by means of a two-stage compressor after being temporally broadened using a grating stretcher. After amplification, the beam was divided between two separate grating compressors to facilitate the pump-probe experiments previously performed with the system. For this study, a single compressor was used. With this system, pulses centered at 800nm could be generated with energies up to 300mJ and temporal durations tunable from 200fs to 10ps.

2.2 Ti:Sapphire Oscillator

A passively mode-locked KM Labs Ti:Sapphire oscillator was used to generate pulses centered at 800nm with FWHM of 40nm at a rep rate of 84MHz. The oscillator was pumped with 4.1W at 532nm using a Millennia eV laser system. A photodiode collecting leakage from one of the output mirrors was used to externally trigger a Stanford Research Systems DG645 delay generator, which provided the timing for the amplification system.

2.3 Chirped Pulse Amplification (CPA) System

In order to perform the experiments described here, it was necessary to achieve pulse powers much greater than the ~5nJ generated by the oscillator. Thus, a two-stage amplification system was used to increase the pulse power to the order of 300mJ for experiments. The schematic layout of the laser amplifier, depicted in Figure 1, consists of four basic structures. First, the pulses are stretched in time to reduce the peak power that the cavity optics must be exposed to during amplification, then the pulses are amplified to 240mJ in a regenerative amplifier (RGA) and a subsequent multi-pass amplifier (MPA), and finally the pulses are temporally recompressed in order to generate output pulses with timescales as short as 200fs. The pump beam (CPA Pump in Figure 1) was provided by a Quantronix Darwin laser system operating at a center wavelength of 532nm. A beam splitter (BS1 in Figure 1) was used to split the pump

between the RGA and the MPA, such that the RGA crystal was pumped with ~3W and the MPA crystal was pumped with ~15W.

2.4 Stretcher

Amplifying femtosecond pulses directly could result in powers high enough to damage even Titanium:Sapphire crystals, so before amplification the beam from the oscillator was directed through a one-grating stretcher to dramatically increase the temporal width of the pulses (and thus decrease their peak power).

2.5 Regenerative Amplifier (RGA)

A Stanford Research Systems DG645 delay generator (DG1) was triggered at 84MHz by the photodiode in the oscillator. The delay generator was set to divide by 84000, so that all channels operated at a 1kHz rep rate. The delay generator was used to trigger the Pockel's cells to let pulses in and out of the RGA cavity. Seed pulses entering the RGA cavity passed through the Pockel cell (PC1 in figure 1) which was held at a voltage to induce a $\lambda/4$ polarization change. Together with the $\lambda/4$ waveplate this results in a $\lambda/2$ polarization as the pulses pass from the thin film polarizer (TFP in figure 1) to the end mirror. Thus, pulses returning to the TFP after a round trip are restored to their original polarization state and are ejected from the RGA cavity by reflection from the TFP. But at a rate of 1kHz, DG1 triggers the Pockel cell driver, which rapidly ramps up the voltage applied across PC1 in order to induce a $\lambda/2$ polarization change. Pulses which pass through PC1 and the $\lambda/4$ waveplate under these conditions experience a $\lambda/2$ polarization change, and are therefore transmitted by the TFP and enter the cavity. Once a pulse has entered the cavity, the driver rapidly decreases the voltage across PC1 so that it once again induces only a $\lambda/4$ polarization on pulses passing through it. During the following time interval (roughly 70ns), the seed pulses arriving from the oscillator every 12ns are rejected by the TFP, while the trapped pulse continues to travel back and forth through the RGA cavity, passing through the TFP because its polarization remains unchanged as it passes through PC1 and the $\lambda/4$ waveplate. The trapped pulse is amplified over the course of ~20 round trips through the Ti:Sapphire crystal that serves as the gain medium. The crystal is pumped at 1kHz by the ~3W portion from the Darwin laser system, with one pump pulse arriving just before each pulse is trapped in the cavity. At a user-defined time, DG1 triggers the Pockel cell driver, which rapidly ramps up the voltage to PC1 again, rotating the polarization as before, and causing the pulse to be reflected from the TFP and directed out of the cavity.

Because of slight timing jitter in the firing of PC1, parts of the pulses preceding and following the selected pulse are also allowed into the RGA cavity and experience amplification. In order to minimize these “satellite” pulses, a second Pockel cell is added (PC2 in Figure 1). When the amplified pulse is ejected from the RGA cavity, PC2 is triggered to rotate polarization of the main pulse by $\lambda/2$, but the timing is set so that the polarization of the satellite pulses is left unchanged. Thus, the satellite pulses are rejected by the Glan-Taylor Prism (GP in Figure 1) and eliminated by the Faraday Isolator (FD in Figure 1). The main pulse passes through GP and into the multipass amplifier (MPA).

2.6 Multipass Amplifier (MPA)

Once a pulse entered the MPA, it was amplified by two passes through the laser medium. BS1 directed $\sim 15\text{W}$ from the pump laser to pump the MPA crystal (TS2 in Figure 1). To increase efficiency, a curved D-mirror after TS2 collects the unabsorbed portion of the pump beam and redirects it back through TS2. The beam from the RGA passes through TS2 as close as possible to the pump path, narrowly missing the flat face of the D-mirror for the pump. After traveling through the multipass amplifier, the amplified beam had a power of $\sim 4\text{W}$.

The MPA output was split into two portions with a 60/40 beamsplitter (BS2 in Figure 1). Part of this was sent to a two-grating compressor inside the Titan laser box. The other portion was compressed separately in an auxiliary compressor. The compression could be easily tuned by using a micrometer to translate a delay stage to alter the path length.

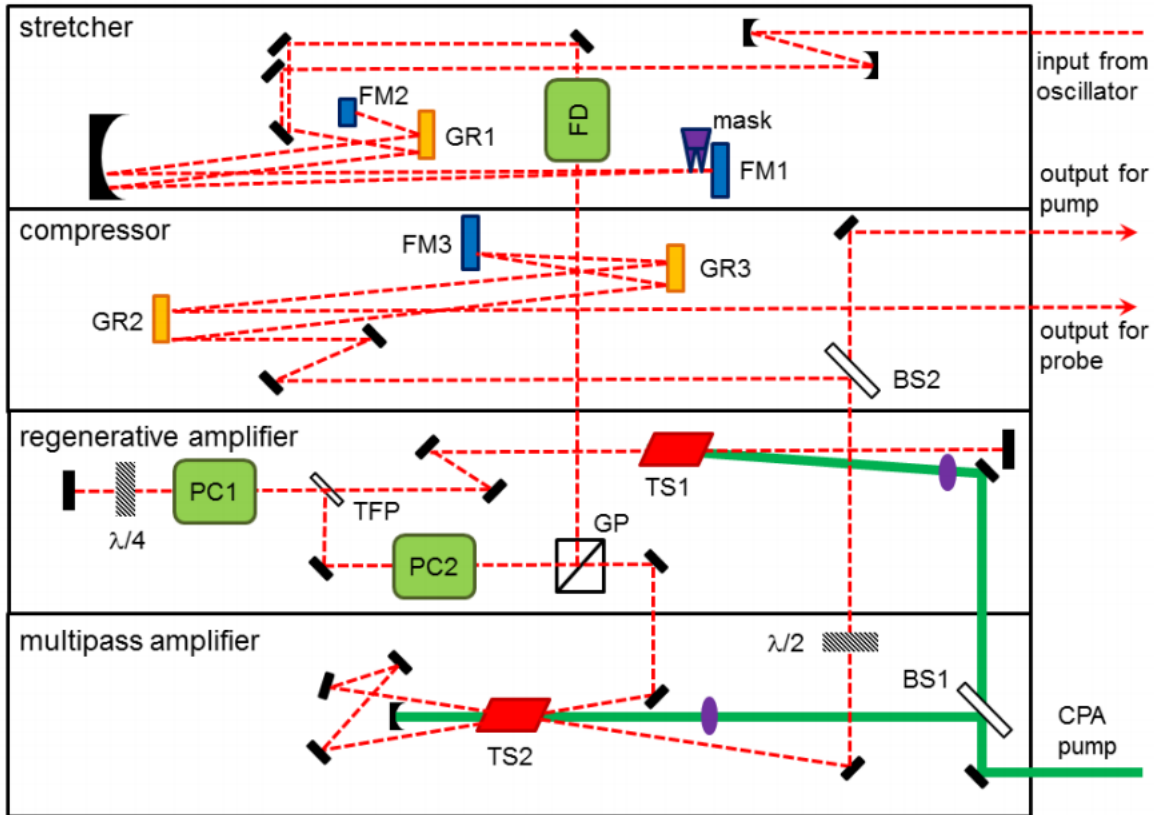


Figure 1: Laser Layout⁴

2.7 Experimental Design

Because the 1ms separation between pump pulses was too short for a mechanical shutter to reliably isolate a single pulse, an optical chopper system (ThorLabs MCxxx) was used to divide the repetition rate down from 1kHz to 200Hz. The 10ps FWHM train of pump pulses was attenuated using a linear gradient neutral density filter, and then focused onto a 1/16" glass slide holding a sample film. The focusing was done with a 20cm focal length lens (L1 in Figure 2). Light from the sample was collected using a camera objective (L2 in Figure 2) and focused into an Andor spectrograph using a third lens (L3 in figure 2). Initial instrument setup and validation was performed by inserting a BBO crystal after the lens to convert the 800nm pump to 400nm which was subsequently focused onto a coumarin-doped PMMA film on a glass sample slide. The excited coumarin produced a blue-green fluorescence, which was collimated and focused into the spectrograph. After validating the concept by the collection of coumarin emission spectra, the BBO crystal and coumarin slide were removed, and a sample slide coated with a Zirconium film was inserted into the sample stage. The compressor was adjusted to yield short pulses (~ 200 fs

FWHM) which generated white light from the glass sample slide after burning through the metal film. The resultant white light beam was easily aligned to the spectrograph and streak camera, as it was bright and was easy to see on a card, even when dispersed inside of the spectrograph. After an initial rough alignment using a card, the streak camera was switched on and the focusing lens in front of the spectrograph was translated in the x, y, and z directions in order to maximize the signal in focus mode. Because the path of the white light was the same as that followed by emission from an ablated metal film, the optimized alignment for white light was subsequently used to collect emission spectra from the ablation of metal films.

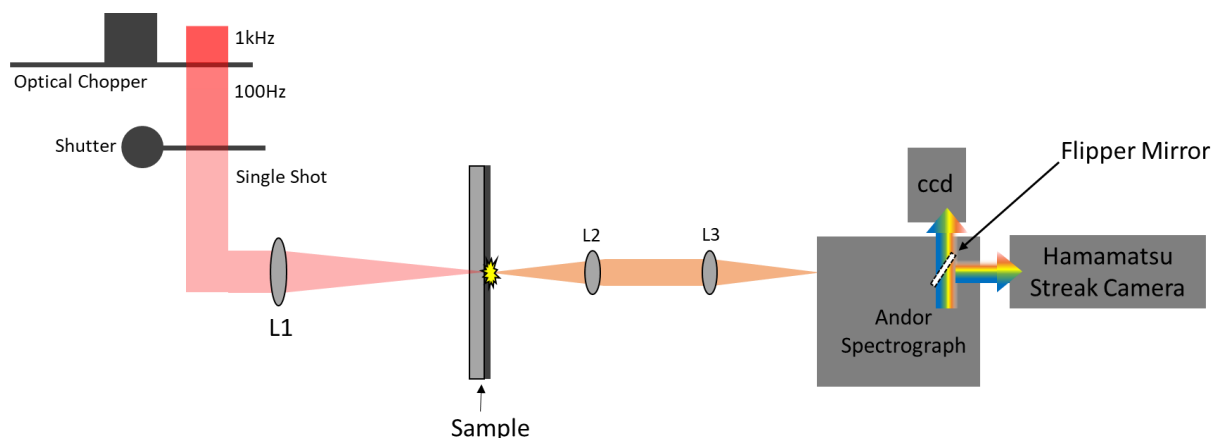


Figure 2: Experimental Layout

2.8 Timing Schemes

Three separate timing schemes were attempted for synchronizing the detection system. All triggering systems used an 84MHz pulse train from the oscillator's photodiode to externally trigger one delay generator (DG1). DG1 was set to divide all channels by 84000 in order to provide a 1kHz rep rate on all channels. The T0 channel was used to trigger the ND:YLF Darwin pump laser used for the Titan CPA system. Because the Darwin system was designed to trigger from the falling edge of the trigger signal, T0 was inverted so that the timing of the falling edge would be independent of the time settings of the other channels. Three of the remaining channels were used to provide the timings for the two Pockel's cells in the RGA. The remaining elements of the timing schemes differ and will now be described individually.

In scheme A (Figure 3), a beam splitter after the chopper was used to direct part of the light to a photodiode. This photodiode then served as the trigger source for a second delay generator (DG2). An inhibit signal, provided by a user-controlled button, allowed output from DG2 only when the button was

pressed, and prevented output otherwise. The frequency of DG2 was divided by two relative to the trigger rate, so as to operate at a frequency of 50Hz. This was necessary, because shutter triggers needed to extend beyond the timing of the next pulse after the inhibit was disengaged, but extension of delays beyond the time of the next clock cycle caused the delay generator to register an error. Delays were set for ~10ms so as to open the shutter for and detect the pulse between clock cycles. But when emission spectra were collected by ablating Zr films with this timing system, the position of the streak varied by ~100ns from shot to shot. The cause of this jitter could not be ascertained, and since it was necessary to acquire in a time range less than 100ns to achieve reasonable resolution, this timing scheme had to be rejected.

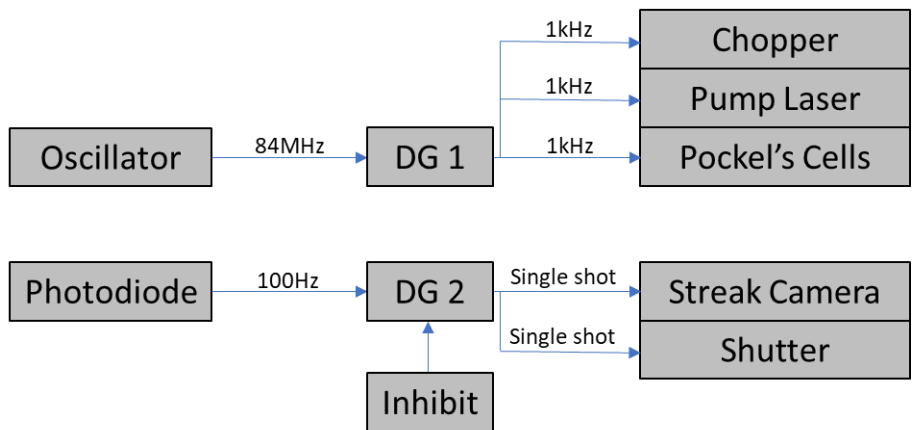


Figure 3: Trigger Scheme A

Trigger scheme B (Figure 4) was similar to scheme A, except that DG2 was triggered at 1kHz from DG1 instead of from a photodiode. In this case, DG2 was set to divide by 20 in order to achieve the desired operation rate of 50Hz described for scheme A. Additionally, because the division performed by DG2 was independent from the division performed by the optical chopper, the timing of DG2 had the possibility of being offset from the timing of the chopped pulse train by some integer number of milliseconds. To correct for this, a photodiode was placed after the optical chopper, and the pulse train measured from the photodiode was displayed on an oscilloscope along with the divided pulse train from DG2. The optical chopper driver was then rebooted repeatedly until the pulse trains were observed to be synchronized. At that point, single pulses were used to ablate Zirconium films, with the emission collected and measured on a streak camera. But as with scheme A, streak camera measurements displayed ~100ns of jitter, rendering this trigger design unacceptable for experiments.

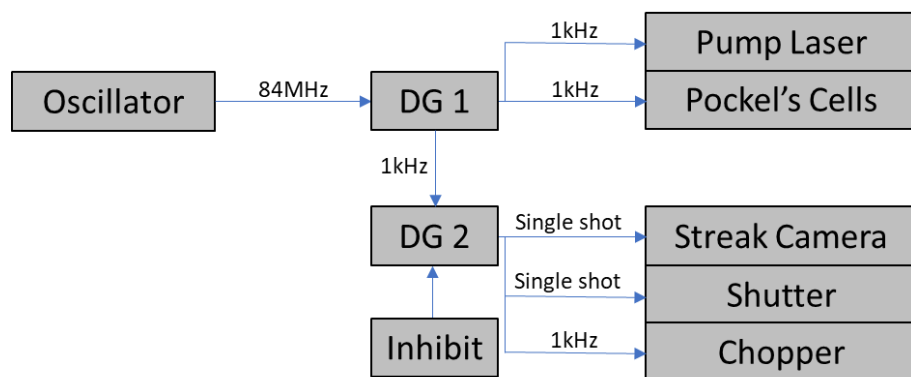


Figure 4: Trigger Scheme B

Trigger Scheme C (Figure 5) was similar to trigger scheme B, except that the streak camera was triggered continuously at 1kHz rather than being provided with a single trigger signal at the time of the laser pulse. As in scheme B, the optical chopper driver had to be rebooted repeatedly until its division was synchronized with that of DG2. The streak camera was operated in sequence mode, in order to collect 20-30 streak images with the timing of each image being based on the timing of the pulses in the 1kHz trigger pulse train. The laser pulse was sent to the sample by means of a manual switch on the shutter control box, which was quickly opened and closed by hand during the acquisition sequence. Although this could allow for several pulses to reach the sample in succession, the spacing between the pulses (10ms) was greater than the time required to fully acquire a single streak image. Thus, by selecting the first image in the sequence which showed signal, it could be ensured that the data corresponded to emission from a single laser pulse. It must be conceded that this system is not ideal. But unlike triggering schemes A and B, it showed negligible timing jitter in the streak images. This made it the only timing system useful for experiments. Consequently, trigger scheme C was used for all experiments.

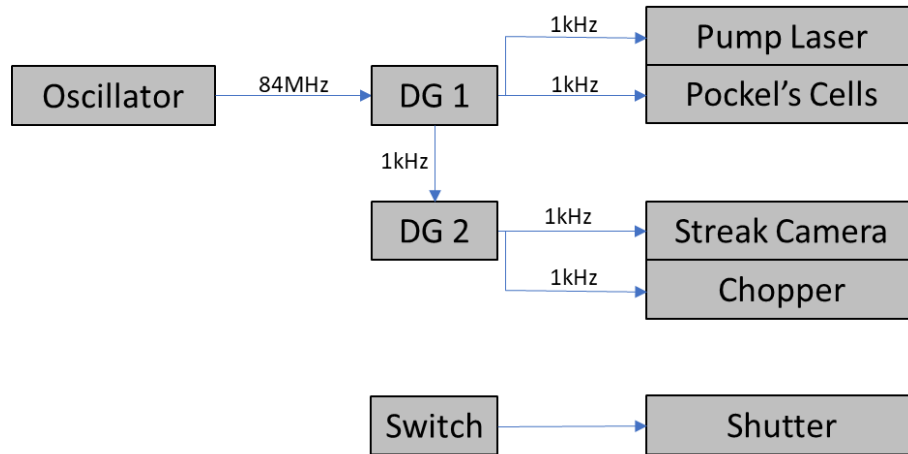


Figure 5: Trigger Scheme C

2.9 Time Profiling

In order to check the pulse duration while adjusting compression, a home-built autocorrelator was used. The incoming beam was initially divided using a beam splitter, with half of the energy being directed to a flat mirror (M2 in Figure 6) and the other half being directed to a retroreflector (RR in Figure 6) mounted on a linear translation stage (TS in Figure 6). The pointing of the incoming beam and the angle of BS were adjusted to achieve a substantial offset between the beams entering and leaving RR. The pointing of M1 was then adjusted to direct the beam through the lens so that it focused on the doubling crystal (Xtal in Figure 6), generating an easily observed 400nm beam. The Xtal was moved to optimize the brightness of the 400nm beam. An additional translation stage was used to facilitate this, but this stage was not strictly necessary. M2 was placed so as to make its distance from BS as close as possible to the distance between RR and BS. The pointing of M2 was adjusted so as to overlap the two focused beams at the crystal. Crude overlap was obtained by observing the spots on a card held in front of the Xtal. At that point, to increase the ease of alignment, the compressor was adjusted to stretch the pulses as much as possible (~ 10 ps FWHM). This will allow temporal overlap of the two pulse trains provided that the two beam paths are within 3mm of the same length. At this point, two separate 400nm spots could be seen on a card placed in front of PD, one generated by each of the two beams. The second harmonic generated by the combination of the two beams should be observed near the middle between these two spots. In order to achieve temporal overlap, TS was translated until a central SHG spot was observed on the card, checking the overlap at the crystal occasionally using a card and making adjustments to the pointing of

M2 as necessary. Once temporal overlap was achieved, M2 was adjusted to maximize the SHG intensity, and M1 was adjusted to direct the central spot to the center of PD. Ideally, the other spots should be widely spaced enough to miss the active region of PD. Finally, a blue filter was added to attenuate any 800nm light that passed through Xtal.

In order to measure pulse durations using this autocorrelator, the PD signal was displayed on an oscilloscope. The intensity of the signal (in Volts) could then be plotted against the delay time in order to determine the autocorrelation function of the pulse. Assuming a Gaussian pulse shape, the FWHM of the laser pulses could be determined by dividing the FWHM of the autocorrelation function by 1.3. The time delay was calculated by doubling the displacement of the delay stage from an arbitrary starting point (to account for the round-trip traveled by the light) and converting this distance to a transit time using the speed of light. To make more rapid measurements, some precision was sacrificed by merely identifying the two delays corresponding to half the maximum intensity, and using these to calculate the FWHM. A typical autocorrelation plot is shown in Figure 7.

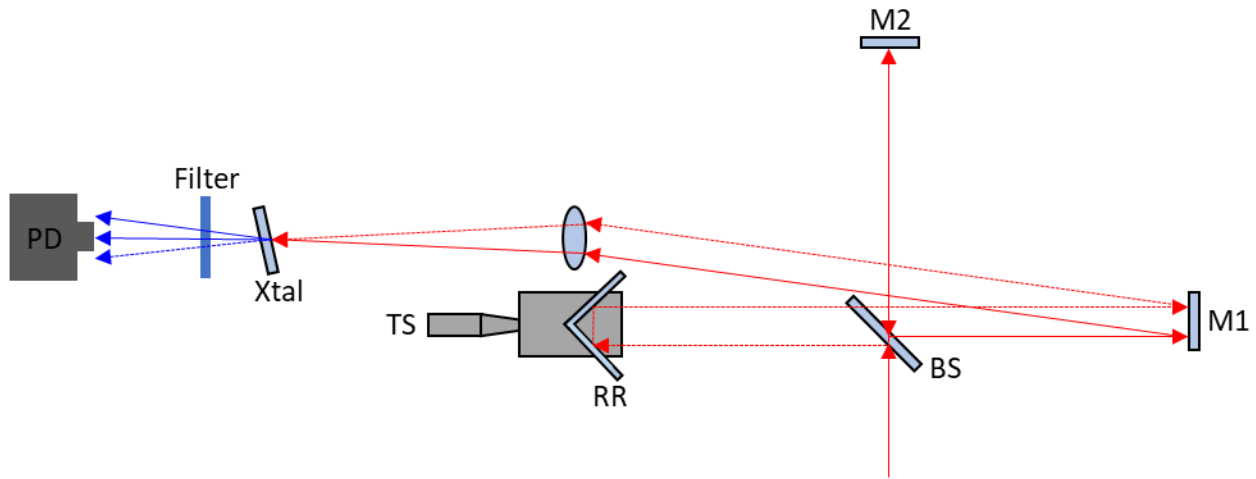


Figure 6: Autocorrelator Layout

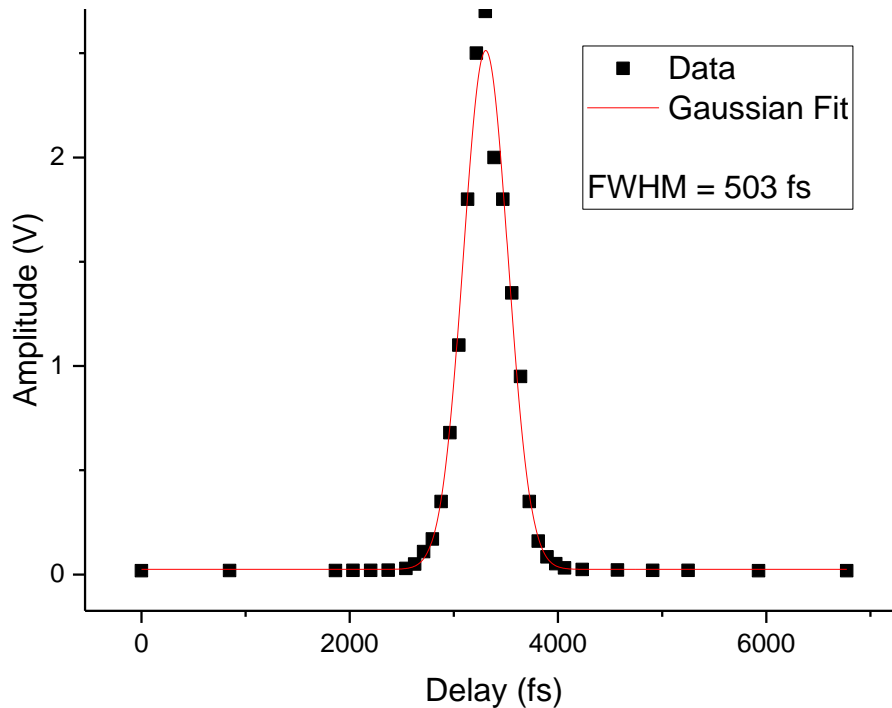


Figure 7: Autocorrelation of Partially Compressed Beam

2.10 Sample Preparation

Samples were prepared by sputtering with an AJA Orion 3 sputter system. Sputtering of Zr was performed at 110W for 17 min (Figure 5) and 25 min (Figure 6). Profilometry was used to determine resultant film thicknesses. The thicknesses achieved were 120nm (Figure 8) and 180nm (Figure 9). Additionally, Al and Mg films with thicknesses ~ 100 nm were prepared for comparison. Finally, Au films prepared by a previous group member were found in a drawer and used to perform comparative measurements.

Besides these, samples consisting of two bilayers of Zn:CuO were prepared by collaborators using sputtering.

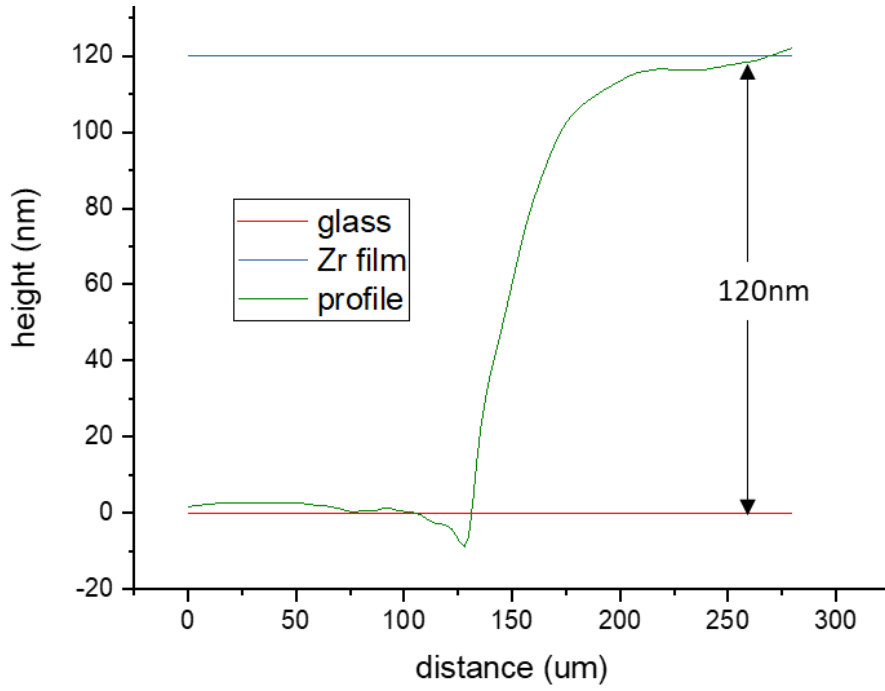


Figure 8: Profile of Thin Zr Film

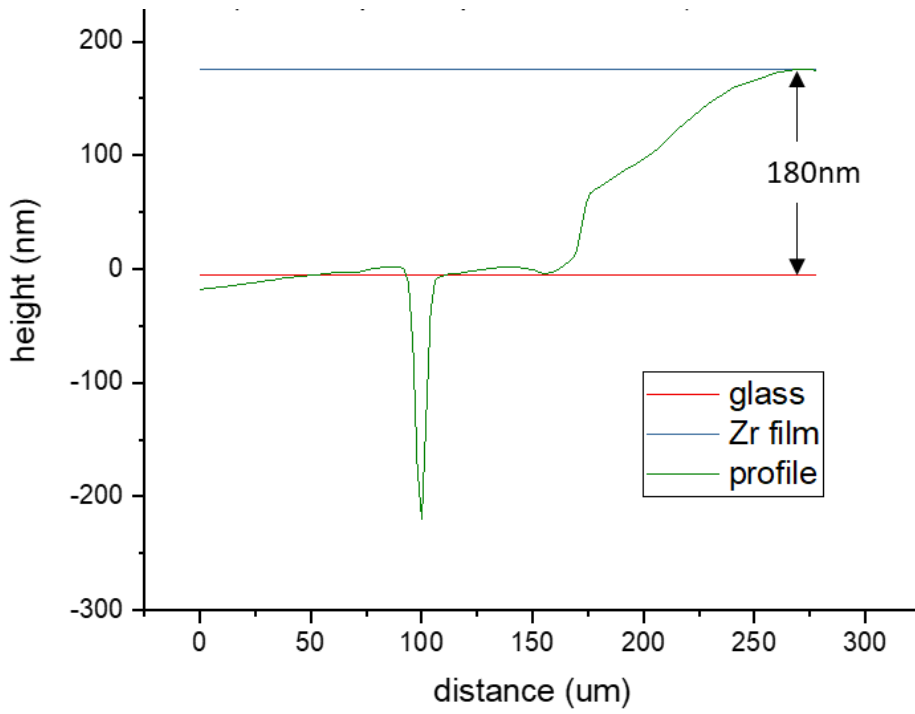


Figure 9: Profile of thick Zr Film

Chapter 3

Results and Discussion

When Zr films were ablated, a jet of sparks was seen to be ejected from the film and extended for ~2cm. When ablation experiments were performed on other metals (Mg, Al, and Au), though, no such spark jets were seen. It is believed that the presence of the sparks in the case of Zr ablation is due to the much lower thermal conductivity possessed by Zr as compared with the others. In order to provide a reasonable comparison of reaction timescales between Zr and other samples, glass slides were clamped to the front of Zr films during ablation to contain the spark jet.

The metal films (Al, Au, Mg, and Zr) were subjected to laser pulses at energies above their respective ablation thresholds, and the resulting emission was detected via the streak camera, as described in the materials and methods section. A typical data set from the streak device, before calibration, is displayed in Figure 10. Such images were obtained for each metal film sample, and the ablation timescales were compared by summing along the spectral dimension and overlaying the resulting temporal profiles in Figure 11. The dip in each profile around 15ns is believed to be due to a burned region on the ccd within the streak device. The longer timescale observed for the thin Zr film is likely due to imperfect clamping of the cover slide, allowing some space for a spark jet.

The thermite samples provided by collaborators were exposed to single laser pulses with powers below, near, and well above the ablation threshold. This resulted in small pinholes in the thermite films which could be seen on a microscope, but the reaction of the thermite did not extend radially from the ablation site to any significant degree. This is in contrast to the results obtained by colleagues when initiating similar samples via laser-driven flyer plates. When initiated by flyer plates, these samples react radially considerably beyond the region actually struck by the flyer plate. The absence of such radial propagation in my system suggests that the presence of radial propagation in the flyer plate initiation system is caused by mechanical forces propagating through the glass slide.

The results obtained indicate that that the spectrometer system constructed is capable of tracking the emission spectra of reacting thermite nanolaminates over time. This information can in turn be used to help in elucidating the mechanism of thermite initiation.

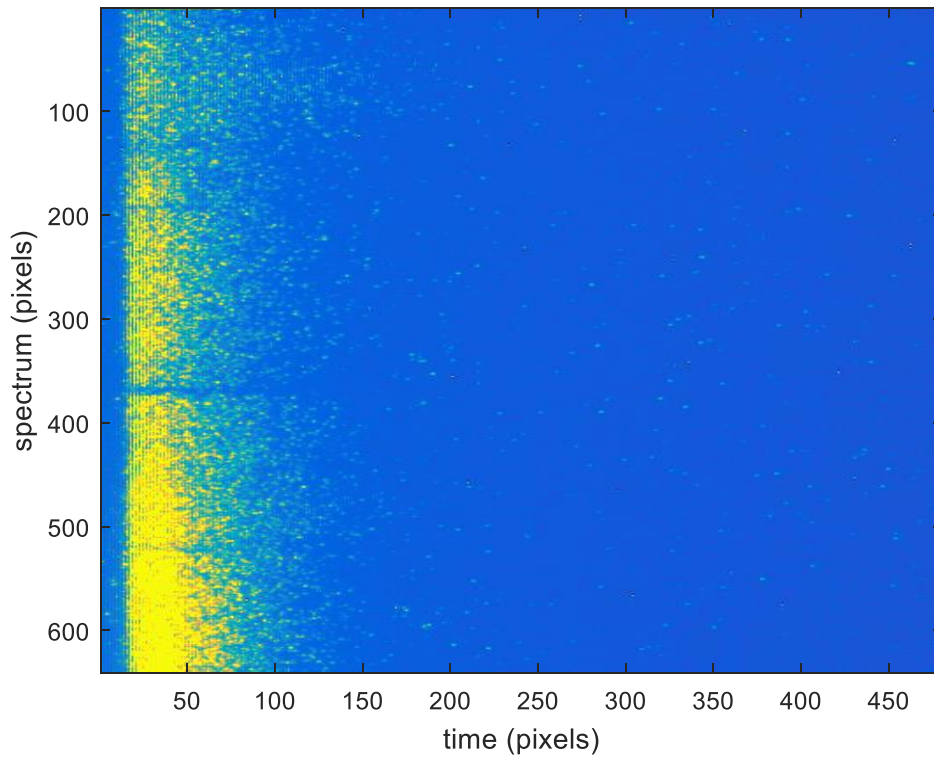


Figure 10: Typical Streak Image

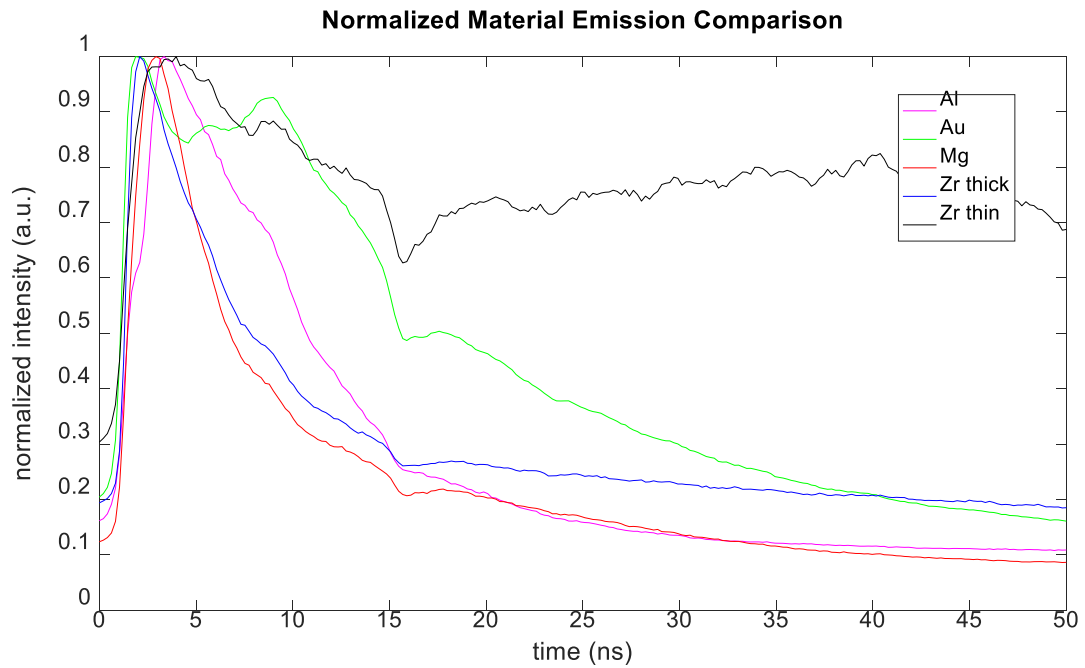


Figure 11: Comparison of Emission Time Profiles

References

1. G. C. Egan, E. J. Mily, J. P. Maria, and M. R. Zachariah, *J. Phys. Chem. C* 119, 20401 (2015).
2. S. M. Matveev, W. P. Basset, D. D. Dlott, E. Lee, J. Maria, *APS Topical Conference on the Shock Compression of Matter*, B2.005, (2017)
3. S. Lu, E. J. Mily, D. L. Irving, J. Maria, D. W. Brenner, *J. Phys. Chem. C* 119, 27587 (2015)
4. C. M. Berg, Doctoral Thesis, *University of Illinois at Urbana-Champaign* (2014)